CAV2021
11th International Symposium on Cavitation
May 10-13, 2021, Daejon, Korea

Numerical Simulation of Vortex Cavitation in a Submerged Impulsive Water Jet by Compressible Mixture Flow Method

Guoyi Peng [1]*, Ryouga Ishitsuka [1], Yasuyuki Oguma [1], Yanbo Peng [2], Hong Ji [2]

[1] Department of Mechanical Engineering, College of Engineering, Nihon University, Japan
[2] College of Energy and Power Engineering, Lanzhou University of Technology, China

Abstract: High-speed submerged water jets have been widely applied but their performance is greatly influenced by unsteady behavior of cavitation clouds shedding. Concerned on the structure of turbulent cavitating flow caused by an impulsively started submerged water jet a numerical investigation is conducted by applying a compressible bubble-liquid mixture flow method, where the mean flow of bubble-liquid mixture is calculated by Unsteady Reynolds Averaged Navier-Stocks (URANS) for compressible fluid. The intensity of cavitation in a local field is evaluated by the volume fraction of gas bubbles whose radius is estimated with the simplified Rayleigh-Plesset equation. Submerged impulsive water jet issued from a short orifice nozzle is treated under the condition that Reynolds number Re = 1.7×10^5 and cavitation number σ = 0.15. The development of turbulent cavitating jet are investigated and the unsteady behavior of cavitation clouds is examined. The reliability of computation method is confirmed by comparison with experiment data. The periodically behavior of cavitation clouds in submerged water jet is captured acceptably.

Keywords: Submerged water jet, cavitation, turbulent flow, compressible bubbly flow, DES

1. Introduction

High-speed water jet injected into still water, which is called submerged water jet, has been received much attention for its capacity of generating very high cavitation impact pressure in the collapse of cavitation bubbles, and widely applied to such as cleaning of mechanical products. Among them submerged impulsive water jet started impulsively can generated a powerful starting vortex ring at the tip of jet. For utilizing the strong impulse pressure caused by starting vortexes water pulse jets are developed and applied in many engineering practices. Until now, many experimental studies have been made concerning jet driven pressure, geometry shape and size of nozzle, cavitation number etc. However, the flow structure of high-speed water jet and unsteady behavior of cavitation clouds included are still unclear for the difficulty to observe the interior of high-speed cavitating flow [1, 2].

Concerned on the flow structure of submerged impulsive water jet a numerical simulation is conducted by using the compressible mixture flow bubble cavitation model [3]. Submerged impulsive water jet (SIWJ) treated is issued from a simple short orifice nozzle, by which an intensive starting vortex with relative high vorticity is expect to be generated. The fluid media of turbulent cavitating SIWJ are treated as a two-phase mixture of liquid and bubble nuclei, which are supposed to disperse uniformly in the liquid. The mean flow of two-phase mixture is calculated by the set of URANS equations for compressible flow and the Detached-Eddy Simulation (DES) turbulence model is applied to evaluate the eddy viscosity. The intensity of cavitation is evaluated by the volume fraction of gas bubbles, whose radius is estimated with the simplified Rayleigh-Plesset equation. The unsteady behavior of cavitation clouds generated in the submerged impulsive water jet is investigated. The temporal distribution of cavitation clouds predicted approximately agrees to experiment data of visualization observation. The phenomenon of periodical shedding of cavitation clouds generated in SIWJ is captured acceptably.

* Corresponding Author: Guoyi Peng, peng@mech.ce.nihon-u.ac.jp

2. Flow governing equations and numerical procedure

2.1 Equations for compressible turbulent mixture flow

The fluid media of cavitating flow are taken as a locally homogeneous two-phase mixture of working liquid and cavitation bubbles. The volume factions of gas phase and liquid are respectively denoted as α_G and α_L. Then, the mixture density ρ is defined as follows by the volume averaging method.

$$\rho = \rho_G \alpha_G + \rho_L \alpha_L \tag{1}$$

Where subscripts *L* and *G* respectively denote liquid and gas phases. A subscript for the mixture is omitted hereafter. The mean flow of mixture is concerned by neglecting the relative motion of liquid and micro bubbles. In consideration of the effect of sharp density variations caused by cavitation URANS equations for compressible turbulent flow are adopted. The variation of temperature is thought to be very small in the whole flow field and the equation of energy is omitted. Then, conservations of mass and momentum for the mean flow of two-phase mixture are written as follows.

$$\frac{\partial \rho}{\partial t} + \boldsymbol{u} \cdot \nabla \rho = -\rho \nabla \cdot \boldsymbol{u} \tag{2}$$

$$\rho \left(\frac{\partial \boldsymbol{u}}{\partial t} + (\boldsymbol{u} \cdot \nabla) \boldsymbol{u} \right) = -\nabla p + \nabla \cdot \boldsymbol{\tau} + \boldsymbol{g} \tag{3}$$

Where $\boldsymbol{u}$ denotes the mean velocity of the mixture, which is treated by neglecting the difference of liquid and gas velocities. $\boldsymbol{g}$ denotes the gravity, and $\boldsymbol{\tau}$ does the stress tensor written as follows.

$$\tau_{ij} = \mu_{eff} \left[\left(\nabla \boldsymbol{u} + \nabla \boldsymbol{u}^T \right) - \frac{2}{3} (\nabla \cdot \boldsymbol{u}) \boldsymbol{I} \right] \tag{4}$$

Where $\boldsymbol{I}$ is the unit tensor. $\mu_{eff} = \mu_m + \mu_{turb}$, denotes effective viscosity that includes both the molecular viscosity μ_m and the eddy viscosity μ_{turb} of the fluid mixture. Here, the mean molecular viscosity is estimated according to the volume fraction of liquid and gas phases [3].

Concerning the eddy viscosity, k-epsilon models and k-omega model are often applied for engineering problems. However they cannot provide accurate results for separated flows with large turbulence scales. In this work, the Detached-Eddy Simulation (DES) approach based on the Realizable k-epsilon model is applied in order to capture small shear vortices and flow separation at the nozzle throat caused by impulsively started high-speed water jet [4]. That is to say, the realizable k-epsilon model is used in the near wall region with application of wall function laws, and it switches into the Large-Eddy Simulation (LES) model in far wall region if the grid spacing is much smaller than the thickness of the turbulent shear layer in all directions.

2.2 Simplified bubbly cavitation model

Concerning cavitation, the compressible mixture flow bubble cavitation model is applied in order consider cavitation phenomenon corresponding to sharp pressure drop. Here the working fluids are treated as a mixture of liquid and bubble nuclei dispersing uniformly. With regarding to the physic property of fluid mixture, both the liquid and gas fluids are supposed to work exponentially, and equations of state for liquid and gas phases are expressed below.

$$\begin{cases} (p + B) / (p_{sat} + B) = \left(\rho_L / \rho_{L,sat} \right)^{n_L}, \quad p_g / p_{g0} = \left(\rho_g / \rho_{g0} \right)^{n_g} \end{cases} \tag{5}$$

Where n denote the specific heat ratio, $p_{L,sat}$ = 2.34 kPa and $\rho_{L,sat}$ = 998.2 kg/m^3, represent the saturation pressure and density of liquid (water) at the reference state when temperature *T*= 293.15 K. The fitted constant *B* = 3.049×10^8 Pa. The gas phase is assumed to be dispersed in the form of micro bubbles, which include both vapor and non-condensation gas. The non-condensation gas treated as perfect one, and the reference pressure and density are taken as p_{g0} = 101.3 kpa and ρ_{g0} = 1.2 kg/m^3

* Corresponding Author: Guoyi Peng, peng@mech.ce.nihon-u.ac.jp

at the given state. Then, the sonic speeds c_L, c_g in liquid and gas media are given as follows.

$$\left\{ \rho_L c_L^2 = n_L \left(p + B \right), \quad \rho_g c_g^2 = n_g p_{g0} \left(R_{b0} / R_b \right)^{3n_g} \right. \tag{6}$$

where R_b denotes bubble radius and the subscript 0 does a reference initial state. Then, by neglecting coalescence and breakup of bubbles the gas volume fraction in per unit mixture volume can be expressed as follows according to N_b, the number of bubbles in per mixture volume.

$$\alpha_G = \left(\frac{4\pi}{3} R_b^3 N_b \right) \left(1 + \frac{4\pi}{3} R_b^3 N_b \right)^{-1} \tag{7}$$

As shown above, the compressibility of gas phase varies with bubble radius. Of course, the oscillation of bubble radius with surrounding liquid pressure may be solved by the Rayleigh-Plesset equation or similar ones. But the calculation of these equations is very time consuming. For the purpose of simplification cavitation bubbles are treated as quasi-still ones in this work and their local mean radius is estimated by solving the simplified Rayleigh-Plesset equation approximately [5].

$$\frac{d R_b}{d t} = Sign(\Delta P) \sqrt{\frac{2}{3} \frac{|\Delta P|}{\rho_L}} \tag{8}$$

Where $\Delta P = p_g + p_v - p$, denotes the pressure difference acting on the bubble surface. This equation is similar to the Schnerr-Saucer model but he the effects of surface tension and non-condensable are taken in to account here via evaluation of the pressure difference bubble inside and outside [6].

2.3 Closing of flow equations

In order to close above equations state equations are used to relate the mixture density and the pressure of continuous liquid phase by referring the mean sonic speed $c_m = (dp/d\rho)^{1/2}$ in the mixture [7]. According to Eq. (1) and Eq. (6) c_M is defined as follows.

$$\frac{1}{\rho\ c_m^2} \cong \frac{\alpha_G}{\rho_g c_g^2} + \frac{\alpha_L}{\rho_L c_L^2} \tag{9}$$

Taking it into eq. (2) we may obtain the following pressure transport equation.

$$\frac{\partial p}{\partial t} + \boldsymbol{u} \cdot \nabla p = -\rho c_m^2 \nabla \cdot \boldsymbol{u} \tag{10}$$

Also, the flowing equation for the gas volume fraction is adopted in consideration of the mass conversation of gas phase.

$$\frac{\partial \alpha_G}{\partial t} + \boldsymbol{u} \cdot \nabla \alpha_G = \alpha_G (1 - \alpha_G) \left(C_{ce} \frac{3}{R_b} \frac{dR_b}{dt} - \Delta \cdot \boldsymbol{u} \right) \tag{11}$$

where C_{ce} denotes a correction coefficient concerning the simplified estimation of bubble radius. Similar to the Schnerr-Saucer model it is taken to be $C_{ce} = 1.45$ when $\Delta P > 0$ and $C_{ce} = 1.25$ when $\Delta P < 0$.

Equations (2), (3), (8, (10) and (11) compose a set of flow governing equations, and they are solved by applying the CCUP (Constraint Interpolation Profile/CIP Combined Unified Procedure) method based on the time splitting technique [8]. The advection phase is calculated by CIP scheme, and the non-advection phase is calculated by the PISO (Pressure Implicit with Splitting of Operators) algorithm [9,10], where the acoustic term is discretized implicitly and the viscous term is done explicitly.

3. Computation Results

Figure 1 (a) shows the submerged water jet system to be concerned, where a short orifice nozzle made of transparent acrylic resin is set up at the side wall of an open water tank, where the depth water

* Corresponding Author: Guoyi Peng, peng@mech.ce.nihon-u.ac.jp

is kept to a given level with an over flow pipe. Pressured tap water from a pressure tank is injected impulsively to the water tank by opening a control valve quickly. The temperature of tape water is 20°C and the initial gas volume fraction is taken to be $\alpha_{G0} = 0.005$. The initial radius of bubble nuclei is taken to be $R_{b0} = 2.5 \times 10^{-6}$ m. The diameter of orifice d = 1.0 mm and the length of throat $l/d = 0.6$. Figure 1 (b) shows the computational domain and structure mesh adopted for the numerical simulation. Focused on the upstream axisymmetric structure the assumption of axisymmetric flow is adopted. The computation domain is taken from -5d upstream of the nozzle inlet to 30d downstream of the nozzle exit. The width of computation domain is taken to be 15d in the radial direction. As for the boundary conditions a given pressure is imposed at the inlet of nozzle inflow pipe according to the specified

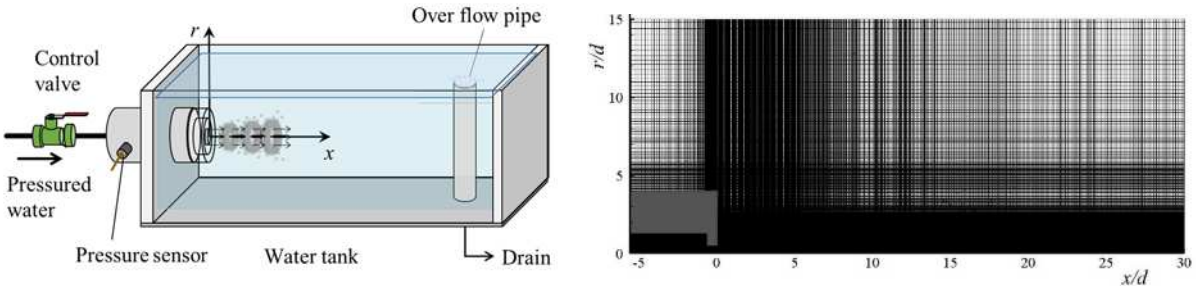

(a) Scheme of water jet device (b) Computational domain and grids

Figure 1. Scheme of submerged water jet and computation domain of numerical simulation.

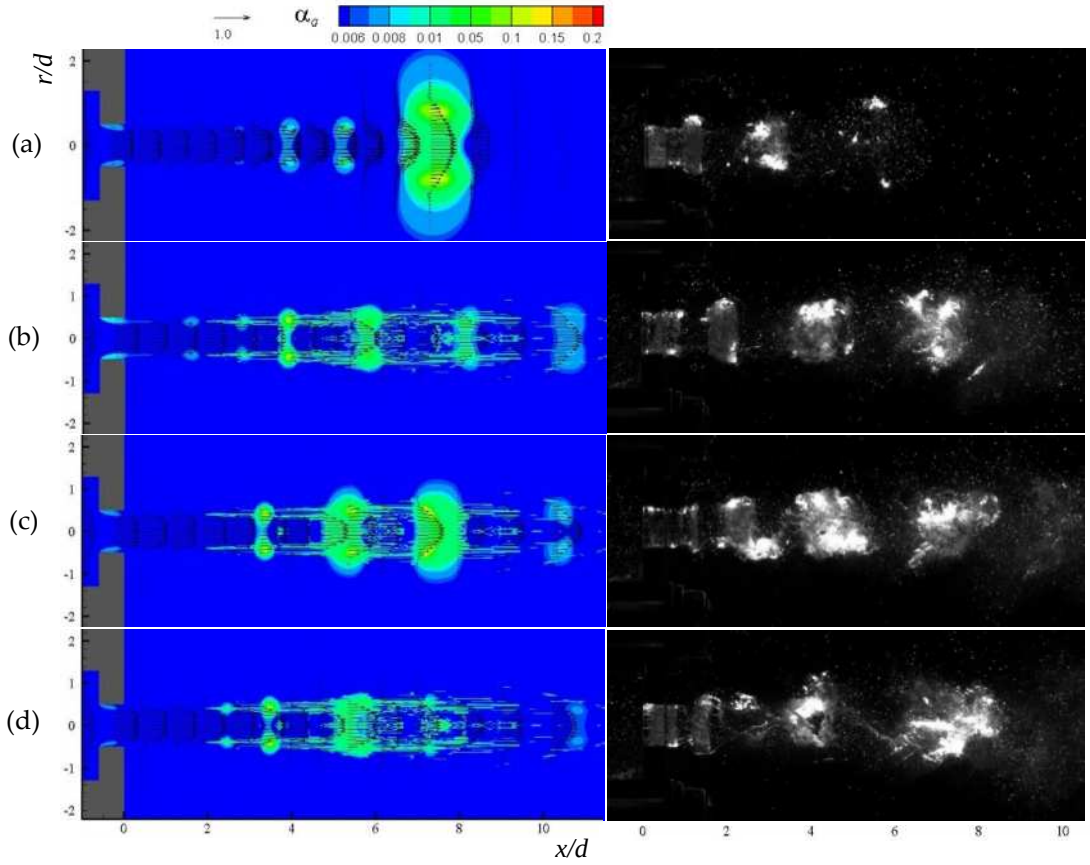

Figure 2. Distribution of cavitation clouds in submerged water jet obtained by numerical simulation (left) and high-speed video camera observation (right): (a) $t = t_1$, (b) $t = t_1 + \Delta t_1$, (c) $t = t_1 + \Delta t_2$, (d) $t = t_1 + \Delta t_3$.

* Corresponding Author: Guoyi Peng, peng@mech.ce.nihon-u.ac.jp

working pressure and the intensity of turbulence is given to be 1.0% of the inflow velocity. At the outlet of right boundary, a given static pressure is imposed and the Neumann condition is applied to other scalar variables. All wall boundaries related to the nozzle are treated as no-slip walls.

As example, Fig. 2 shows instantaneous distributions of gas volume fraction and velocity victors of computation results, where the injection pressure $P_{in} = 0.6$ MPa and the discharge pressure $p_o = 0.1$ MPa. Thus, the cavitation number $\sigma \cong 0.15$ and the Reynolds number $Re \cong 1.7 \times 10^5$. The red color denotes gas phase and the blue one does the liquid phase. The area demonstrated by yellow and green colors present axial section of cavitation clouds, where the value of α_G is relatively high. The dark vectors denote the mean velocity in local flow field. Figure 2 (a) shows the flow distribution when the starting vortex ring is getting to disperse, where cavitation clouds appear at the center of starting vortex and on the shear layer behind the starting vortex. Flow observation shown on the right of Fig. 2 (a) demonstrates that the starting vortex ring collapses near $x/d = 6$ but it is not presented correctly by the numerical simulation since the two-dimensional axisymmetric assumption is adopted here. Figure 2 (b)~(c) shows periodic sheading of cavitation clouds when the jet is well developed, where Fig. 2 (b) demonstrates velocity vector distribution and generation of cavitation clouds on the shear layer near to the nozzle exit. Figure 2 (c) does the flow distribution when cavitation rings are expanding to big ones approaching to collapse. Figure 2 (d) does the flow distribution just when the developed cavitation rings collapsed, where cavitation rings broken down at the downstream. For comparison, photographs of visualization observation taken by high-speed video camera under the same working condition are shown on the right, where the appearance of cavitation clouds is demonstrated by a sequence of pictures taken at imaging speed of 5,000 fps. These pictures were taken under leaser sheet light projecting condition, and the area of cavitation clouds are observed to be bright for reflection of light at cavitation bubble surfaces within the laser sheet width. Comparing computational and experimental results shown in the figure we note that vortex cavitation rings near to the nozzle are predicted acceptably but the collapsing of cavitation clouds at the downstream is not presented correctly. The reason may be mainly concluded to the influences of 2D axisymmetric assumption. The capability of present cavitation model to capture unsteady vortex cavitation is demonstrated although further verification is required. The temporal distributions of gas volume fraction predicted approximately agree with the experimental results of high-speed camera observation.

4. Conclusions

Numerical simulation of submerged impulsive water jet has been performed by using the simplified compressible mixture flow bubble cavitation model in order to clarify the unsteady behavior of cavitation clouds. The reliability of computation method is confirmed by comparison with experiment data.

Computation results confirms that cavitation initially appears near the wall at the nozzle throat and then vortex cavitation occurs on the shear layer around jet. The possibility to capture the periodical shedding of cavitation clouds by present method is confirmed although further verification is required.

References

1. Kalumuck, K.M., Chahine, G.L. The use of cavitating jets to oxidize organic com-pounds in water, J. Fluids Eng. 2000, 122, pp.465-70.
2. Nishimura, S. et al. Similarity law on shedding frequency of cavitation cloud induced by a cavitating jet, J. Fluid Sci. & Tech. 2012, 7(3), pp.405-20.
3. Peng, G. et al. Numerical analysis of cavitation cloud shedding in a submerged water, J. Hydrodynamics (B), 2016, 28(6), pp.986-93.
4. Constantinescu, G. et al. Detached-Eddy Simulation of flow over a sphere, AIAA Paper 2002, 2002-0425.
5. Peng, G. et al. Numerical simulation of unsteady cavitating jet by a compressible bubbly mixture flow method, IOP Conf. Series: Earth and Environmental Science, 2018, 163, 012037.

* Corresponding Author: Guoyi Peng, peng@mech.ce.nihon-u.ac.jp

6. Yamatomo, Y. et al. A simple cavitation model for unsteady simulation and its application to cavitating flow in two-dimensional convergent-divergent nozzle, IOP Conf. Ser.: Mater. Sci. Eng. 2015, 72, 022009.
7. Park, S. and Rhee, S.H., Comparative study of incompressible and isothermal compressible flow solvers for cavitating flow dynamics, J. Mech. Sci. Tech., 2015, 29(8), pp.3287~96.
8. Peng, G. et al. An improved CIP-CUP method for submerged water jet flow simulation, JSME Int. J. (B), 2001, 44(4), pp.497-504.
9. Seif, M.S. et al. Implementation of PISO algorithm for simulating unsteady cavitating flows. Ocean Engineering, 2010, 37, pp.1321–1336.
10. Miller, S.T. et al. A pressure-based compressible two-phase flow finite volume method for underwater explosions. Computers & Fluids. 2013, 87, pp.132–143.

* Corresponding Author: Guoyi Peng, peng@mech.ce.nihon-u.ac.jp